International Journal of Heat and Mass Transfer 159 (2020) 120076

Contents lists available at ScienceDirect

International Journal of Heat and Mass Transfer

journal homepage: www.elsevier.com/locate/hmt

Spreading and bouncing of liquid alkane droplets upon impacting on a heated surface

Mengxiao Qin[a,b], Yang Guo[a], Chenglong Tang[a,*], Peng Zhang[b], Zuohua Huang[a]

[a] State Key Laboratory of Multiphase Flows in Power Engineering, Xi'an Jiaotong University, Xi'an, 710049, China
[b] Department of Mechanical Engineering, The Hong Kong Polytechnic University, Hung Hom, Kowloon, Hong Kong

ARTICLE INFO

Article history:
Received 14 January 2020
Revised 7 June 2020
Accepted 11 June 2020
Available online 22 June 2020

Keywords:
Hydrocarbon droplet impact
High temperature
Rough surface
Spreading diameter
Residence time

ABSTRACT

This paper reports an experimental investigation on the impact dynamics of liquid normal alkane (n-heptane, n-decane and n-tetradecane) droplets on a stainless steel surface using high speed photography and long distance microscopic techniques. Particular interest is paid to comprehensively explore the effects of liquid viscosity and surface roughness on droplet spreading and bouncing dynamics at different thermal hydrodynamic impact regions. Specifically, firstly, high speed images identified four regimes (evaporation, nucleate boiling, transition boiling and film boiling regime) of physical phenomena that couple the droplet spreading hydrodynamics, heat transfer and phase change. Bubbles generation due to the heating of the surface with compression of air disk under the droplet was observed and this phenomenon is firstly promoted and then inhibited with the increase of the wall temperature until finally no bubbles were observed when wall temperature is beyond the Leidenfrost point (T_L). Rim disturbances during spreading were observed at relatively high Weber number with wall temperature higher than T_L. Increasing wall temperature reduces the rim disturbance. Secondly, the measured non-dimensional maximum spreading diameter β_{max} decreases with the increase of surface temperature until it becomes a constant when temperature is beyond T_L. Rough surface was found to have a lower T_L because of larger vapor pressure provided by more nucleation sites. Finally, for wall temperature beyond T_L, droplet bounces up after a certain period of residence time (τ_r). It takes more time for droplet to rebound at larger *We* because of larger β_{max} takes longer time to retract and rebound. Both surface roughness and liquid viscosity showed no influence on time to reach β_{max} (τ_{max}), but significantly increases τ_r by slowing the retracting process, which both should be considered in future model of τ_r.

1. Introduction

Droplets impacting on a heated surface is a concern in combustion engines, spray cooling, and even prevention of blade erosion in gas turbines. The impact phenomenon is significantly complex as it is governed by the coupled physics of heat transfer, phase change and hydrodynamics. In addition, the heat transfer rate is non-monotonic with increasing the surface temperature, as shown by the Nukiyama curve [1]. Generally, four regimes in terms of the heat transfer rate have been identified [2–4]. In the droplet evaporation regime where the surface temperature T_w is below the liquid boiling temperature T_b, the impact dynamics is similar to that at cold surface but is affected by the temperature-dependent surface tension. When T_w increases to a value beyond T_b, nucleate boiling occurs, and isolated vapor bubbles generated at the contact surface rise to the liquid air interface; this is called nucleate boiling regime. The heat transfer rate reaches its maximum at a critical heat flux temperature T_C which is also called the "boiling crisis" point. Further increasing surface temperature reduces the heat transfer rate, because the vapor bubbles are generated and merge to form larger ones or even a vapor film so that the droplet partially contacts the surface; this regime is called the transition regime. If the temperature is further increased to above the Leidenfrost temperature, T_L, the stable vapor film prevents the droplet from contacting the solid surface completely so as to reduce the heat transfer rate to a minimum; this is the film boiling regime or Leidenfrost regime.

Although there is general consensus on the sequential occurrence of these four regimes with increasing T_w, most of the previous experiments were performed with a given liquid and surface. The critical points, such as T_L and T_C on the boiling curve, depend

* Corresponding author: Dr Chenglong Tang, Xi'an Jiaotong University, State Key Laboratory of Multiphase Flows in Power Engineering, NO 28 WEST XIANNING ROAD, Xi'an 710049, China.
E-mail address: chenglongtang@mail.xjtu.edu.cn (C. Tang).

https://doi.org/10.1016/j.ijheatmasstransfer.2020.120076
0017-9310/

on the impact condition [5], surface roughness [6] and environment [7]. The transition boundaries of water droplets on heated polished aluminum surface between different impact regimes were discussed by Bertola [8]. Three regimes were identified and transitions between different regimes were discussed by Tran et al. [9].

The maximum spreading diameter of droplet, which is usually normalized by the droplet initial diameter to yield β_{max}, is an important parameter to describe the droplet impacting dynamics on a solid surface, especially to understand the film thickness and heat transfer behaviors during the spreading. Many studies have been devoted to understanding various factors affecting β_{max}, such as the impact velocity [10], liquid viscosity [11] and surface roughness [12]. Several correlations of β_{max} in film boiling regime have been proposed [9, 13, 14], which are usually considered to be only *We* dependent.

As a concomitant quantity of droplet spreading, the residence time τ_r, which is defined as the time between the droplet impact on the surface to the droplet rebound from the surface, is also crucial for the heat transfer upon droplet impacting a heated wall. The residence time was found to decease with increasing the impact velocity on both smooth and rough surface [12]. The hydrophilic surface treatment was found to remarkably reduce the drop-solid contact angle and results in decreased residence time [15]. The contact time was found almost independent of the impinging angle [10]. The increase of droplet diameter leads to rapidly increased contact time [10].

From an engineering point of view, one prominent example related to droplet impingement is the mixture formation process in confined chamber of the internal combustion engine. The total fuel efficiency of an engine is affected if the fuel droplet is deposited on the chamber wall and not fully evaporated, which contributes to the emission of unburned hydrocarbon as well. Second, the evaporation of the secondary droplets generated from either the hydrodynamic splashing or the nucleate/film boiling may influence the near wall mixture formation and also the unburned hydrocarbon emission. Finally, accurately embedded sub-models of droplet impact is necessary for modeling spray impingement process in engines.

Surface structure not only influences β_{max} when the surface is cold but also is important when a droplet impacts a heated surface. Surfaces with micro-structures of different sizes and shapes were found to enhance heat flux during spray cooling. Central jet phenomena was found to occur only on micro-patterned surface [16]. Most works on droplet/high temperature wall impact use smooth or textured surfaces. It is expected that rough surface provides more nucleate cites during the spreading, and consequently affects the heat transfer behaviors during the interaction process. However, the influence of surface roughness has not been sufficiently explored. In addition, previous models for maximum spreading diameter and residence time in the film boiling regime also are proposed without consideration of surface roughness. Furthermore, viscosity is an important property of liquid and significantly influences the spreading dynamics in droplet impact when the surface is not heated [17]. The difference of viscosity between varied liquids is believed to be decreased when the surface is heated, thus the liquid viscosity effect is not considered in the modeling maximum spreading diameter and residence time [18, 19]. However, experimental verification of this handling is still required.

As such, in this work, droplet impact behaviors on heated surfaces were experimentally investigated, by using different alkane droplets with varying viscosity and impact inertia. Smooth and rough surfaces with elevated temperatures were used. Firstly, high speed microscopic techniques will be used to capture the transient impact behaviors at typical thermo hydrodynamic regimes with high time and space resolution such that bubbles generated by the heating of the surface and droplet spreading rim disturbances at varied surface temperature will be examined. In addition, time resolved droplet spreading diameters with its maximum value for different wall temperatures, liquids properties and Weber numbers will be measured for both the smooth and roughed surface. Finally, in the film boiling regime where the wall temperature is higher than the Leidenfrost point, the maximum spreading diameter and residence time for droplet at varied surface temperature with different liquid properties and surface roughness will be analyzed.

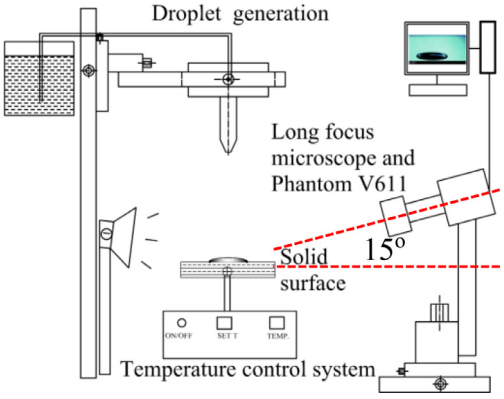

Fig. 1. Sketch of the experimental system of droplet impacting a heated surface.

2. Experimental specifications

2.1. Experimental setup

Fig. 1 shows the schematic of the experimental set-up that allows us to observe and distinguish the different regimes of droplets impacting the heated surfaces. The experimental system consists of the droplet generation system, the high- speed imaging system, the solid surface and heating device. Droplets are generated at the tip of a hypodermic needle (inner diameter = 0.45 mm, 26 G) mounted on a three-dimensional positioner and falls down vertically under its own weight onto the horizontal, dry, stainless steel surface. The droplet impact process was recorded by a Phantom V611 high-speed camera, attached by a long focus microscope and operated at 10,000 fps; the resolution of the recorded video is 100 pixel/mm. The camera is tilted to get more information of the droplet in horizontal direction. The droplet release height H is adjustable, and the velocity before impact can be obtained from the high- speed video. The experiments were conducted in an environment at room temperature (20 °C) and atmospheric pressure.

The heating device, HP-1010, was equipped with a thermostat. As a consequence, its topmost aluminum surface (100 × 100 mm in size) can be well maintained as the constant heating temperature with an accuracy ± 0.1 °C. Power of the heating device is 300 W and the highest aluminum wall temperature can reach 600 °C.

2.2. Characterization of droplets and surfaces

The liquids studied in this work include n-heptane, n-decane and n-tetradecane. The physical properties of these liquid normal alkanes are presented in Table 1 [20]. The liquids have very similar surface tension and density but quite different viscosity and boiling point temperatures (T_S). The droplet diameter is fixed at 1.95±0.03 mm. By adjusting the height between the syringe and surface, the impact velocity U_0 can be varied between 0.45 and 1.1 m/s, resulting the Weber number $We=\rho D_0 U_0^2/\rho$, ranging from 20 to 70, and Ohnesorge number $Oh = \mu/(\rho\sigma D_0)^{1/2}$ ranging from 0.0025 to 0.0110, where ρ is the density of fluid, U_0 is the impact

Table 1
Physical properties of the tested liquids at 1 atm and 20 °C [20].

Liquid	σ (N/m)	μ (mPa•s)	ρ (g/cm^3)	boiling point (°C)	*Oh*
n-heptane	0.0204	0.41	0.680	98.4	0.0025
n-decane	0.0243	0.92	0.730	174.2	0.0049
n-tetradecane	0.0265	2.18	0.767	254.0	0.0110

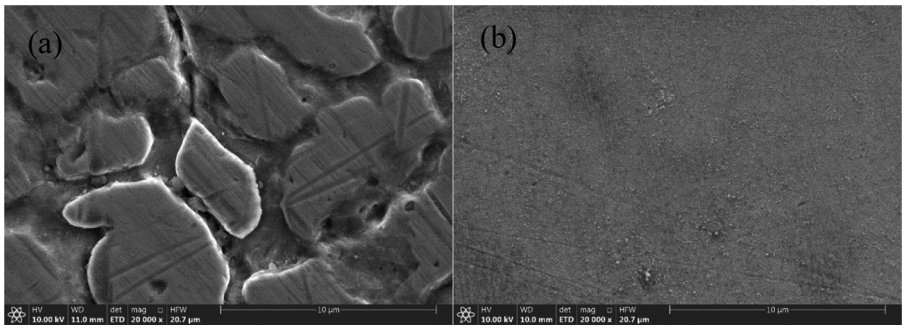

Fig. 2. Scanning electron microscope (SEM) images of (a) the rough surface and (b) the smooth surface.

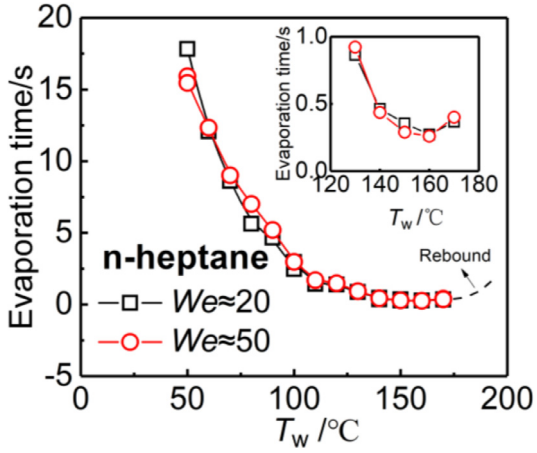

Fig. 3. Evaporation time of n-heptane droplet on heated smooth surface at *We* ≈ 20 and 50.

velocity of droplet, D_0 is the diameter of droplet, σ is the surface tension of fluid, μ is the viscosity of fluid.

The surfaces used in this work are two stainless steel surfaces with different roughness acquired from the manufacture (Shanghai Haocheng Metal Material Company, Ltd. China). Fig. 2 shows the scanning electron microscope (SEM) images of the surfaces. The surface roughness is R_a = 0.1 μm for the smooth surface (mirror, 8k) and 5μm for the rough surface (SS 304). The surface is heated from 30 °C to 500 °C in this work and cleaned by ethanol after each experiment. The reliability of the cleaning procedure was double checked. The spreading diameter evolution and the maximum spreading diameter for repeated experiments are found to be exactly the same after cleaning.

The evaporation time is defined as the time from the impact of the droplet on the surface to the time when the droplet is fully evaporated. The evaporation time of n-heptane at *We* ≈ 20 and 50 is presented in Fig. 3. It takes shorter time for the droplet to completely evaporate at higher surface temperature (T_w) in evaporation and nucleate boiling regime. The droplet have shortest evaporation time in the critical heat flux point (T_C), which is 160 °C for n-heptane. Then the evaporation time is slightly increased as presented in the inset figure in Fig. 3 in the transition regime until the dynamic Leidenfrost temperature is reached (180 °C for n-heptane at *We* ≈ 20 and 50). It's noted that the evaporation time is not able to be measured in this experiment because in this film boiling regime, the droplet rebounds completely and jumps out of high-speed camera view of window.

3. Results and discussion

3.1. Phenomenological description

3.1.1. Thermal hydrodynamic impact regions at various We and roughness level

As a representative case, Fig. 4 shows an n-heptane droplet impacting the heated smooth surface at *We* ≈ 20. At a relatively small T_w = 30 °C, as seen in Fig. 4(a), the droplet spreading is almost the same with that on a cold surface because the T_w is slightly higher than the environmental temperature so that the vaporization is minimal. The droplet reaches its maximum spreading diameter β_{max} ($\beta_{max} = D_m/D_0$) at 8.5 ms, and the lamella recoils afterwards. The recoil is promoted with the increase of T_w, since at T_w = 110 °C, as shown in Fig. 4(b), the recoiled diameter at 22.0 ms is much smaller than that at 25.3 ms for T_w = 30 °C.

At T_w = 130 °C, which is higher than the boiling temperature T_b = 98 °C of n-heptane, as shown in Fig. 4(c), some bubbles are formed inside the droplet by nucleate boiling. Enlarged images of droplets at *We* ≈ 50 where the bubbles in the droplet are more conspicuous, are presented in Fig. 7. Multiple secondary droplets are ejected from the droplet during its recoiling due to the high rate of heat transfer from the surface and consequent growth of vapor bubbles.

As we have discussed in Section 2, there is a critical surface temperature T_C at which the boiling is the strongest and the evaporation time is the shortest. It is found that T_C = 160 °C at *We* ≈ 20 for n-heptane as already presented in Fig. 3. Further increase of the T_w weakens the boiling because the heat transfer enters the transition boiling regime and large vapor bubbles are generated under the lamella as presented in Fig. 4(d). It is noted that the contact angle is larger than 90° at 4.5 ms, which indicates the wetting-to-non-wetting transition by increasing the T_w; this is a universal phenomenon for all the cases. Furthermore, due to the partial non-wetting and therefore less energy dissipation, the receding lamella gains more kinetic energy and forms a column, which tends to bounce away from the surface at 30 ms.

At T_w = 190 °C, which is higher than the dynamic Leidenfrost temperature T_L = 180 °C for n-heptane at *We* ≈ 20, as shown in Fig. 4(e), film boiling occurs, and no secondary droplets were ob-

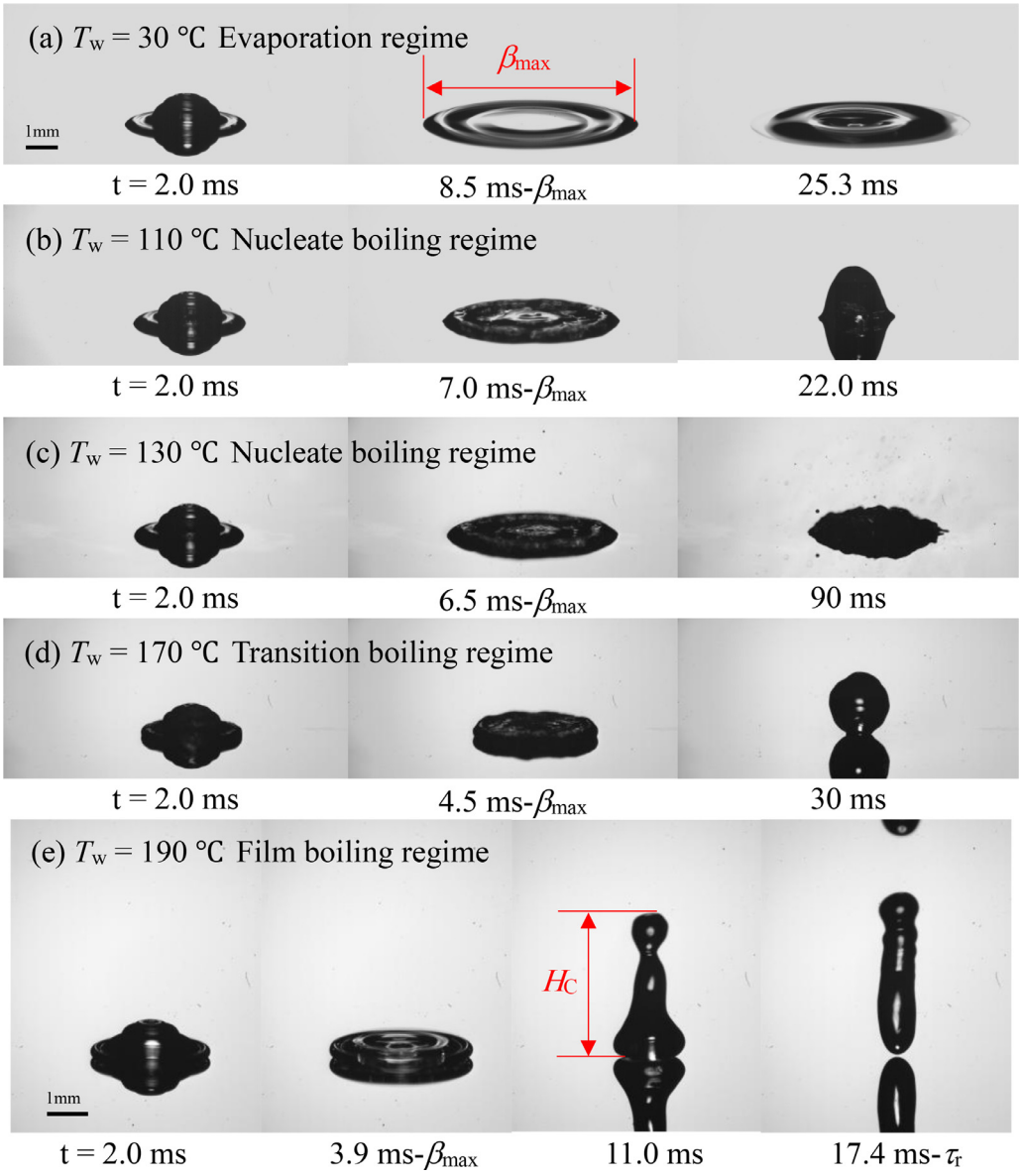

Fig. 4. Typical images of n-heptane droplets at *We* ≈ 20 on smooth surface in different regimes.

served. This is because the formation of Leidenfrost gas cushion insulates heat transfer from the surface to the droplet. The droplet is supported by a developing vapor layer whose thickness is several orders of magnitude smaller than the droplet initial diameter [19], and it bounces off after a short period of time at 17.4 ms defined as residence time τ_r.

Fig. 5 shows images of n-heptane droplet at *We* ≈ 20 impact on rough surface at T_w = 170 °C. Different from cases on smooth surface, the droplet has already reached film boiling regime on rough surface, the droplet bounces at 18 ms after reaching the maximum spreading diameter at 3.8 ms, which is a little bit longer compared to the residence time on smooth surface.

3.1.2. *Bubble formation at various* Weber number *and roughness level*

When T_w is higher than the liquid boiling point, isolated vapor bubbles are generated at the contact surface. Images of the bubbles formation in the n-heptane droplet impacting the smooth surface at *We* ≈ 50 and T_w = 110 °C are shown in Fig. 6. There are small bubbles generated in a circle because of the heating of the surface at 1.0 ms by nucleate boiling as marked by a red arrow. A bubble in the center appears at 1.1 ms because of the contact of air disk with the surface under the droplet [21] as marked by the red arrow. During the spreading, the part of the lamella with bubbles is thinner and evaporated faster at 7.8 ms which looks like a wheel hub.

Fig. 7 shows the bubble formation of n-heptane at *We* ≈ 50 and 1.0 ms with different T_w. Firstly, images of the droplet at T_w = 30 °C that with only one bubble formed in the middle because of the compress of the air disk [21] during spreading. At T_w = 80 °C, the n-heptane droplet reaches the boiling point, a circle of multiple small bubbles is observed. At T_w = 130 °C and T_w = 170 °C, much more bubbles are formed because of higher heat transfer due to the increase of T_w. At T_w = 190 °C and T_w = 300 °C, the droplet impact is in film boiling regime and no bubbles but a thin gas film under the droplet are formed.

Fig. 8 shows bubble formation of n-tetradecane droplet on smooth and rough surface at different T_w. At T_w = 265 °C, a circle of small bubbles formed because heating at T_w higher than T_S (the boiling point for n-tetradecane is 254 °C) is in nucleate

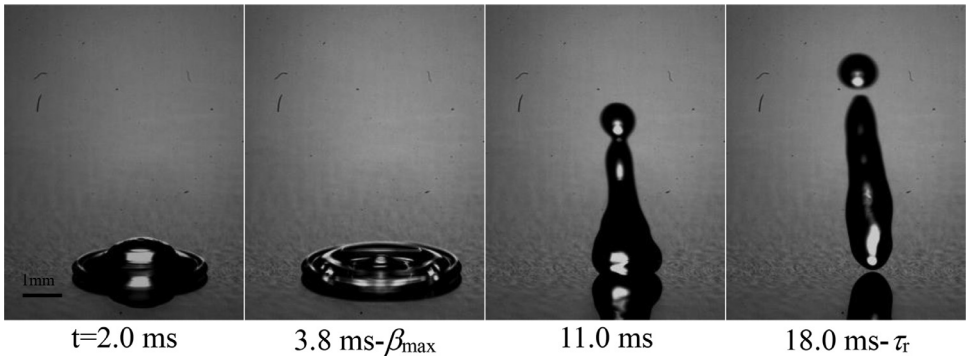

Fig. 5. Typical images of n-heptane droplets at $We \approx 20$ on rough surface at $T_w = 170$ °C.

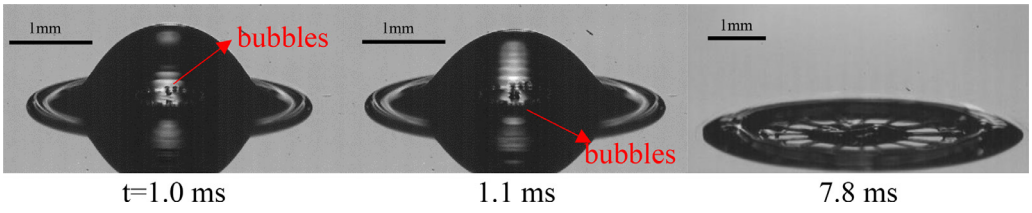

Fig. 6. Enlarged images of bubbles formed in the n-heptane droplets during spreading at $We \approx 50$ at $T_w = 110$ °C on smooth surface.

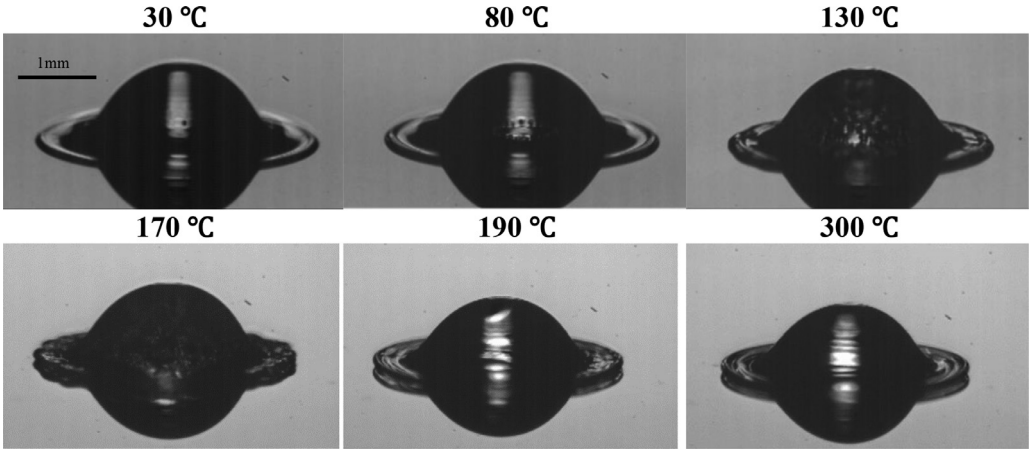

Fig. 7. Enlarged images of bubbles formed in the n-heptane droplets during spreading at $We \approx 50$ at 1.0 ms on heated smooth surface with different T_w.

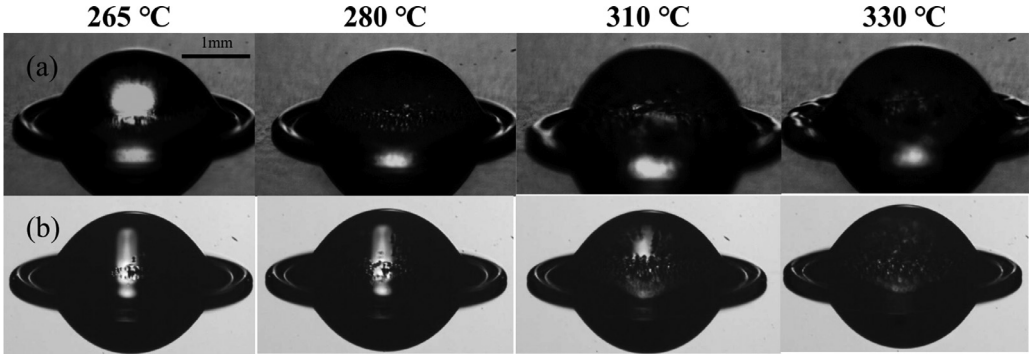

Fig. 8. Enlarged images of bubbles formed in the n-tetradecane droplets during spreading with different T_w at $We \approx 70$ at 0.9 ms. (a) rough surface; (b) smooth surface.

boiling regime both on smooth surface and rough surface. Then at $T_w = 280$ °C, multiple bubbles are generated on rough surface while there is still only a circle of small bubbles formed on smooth surface. At $T_w = 310$ °C and 330 °C, multiple droplets with larger sizes are generated on smooth surface while much more bubbles are formed for droplet on rough surface. In conclusion, larger surface roughness provides more nucleation sites and leads to more and larger bubbles at the same time and T_w.

3.1.3. *Rim disturbance at various We, Oh, and roughness*

Fig. 9 shows images of n-heptane, n-decane and n-tetradecane droplet spreading on smooth and rough surface above Leidenfrost

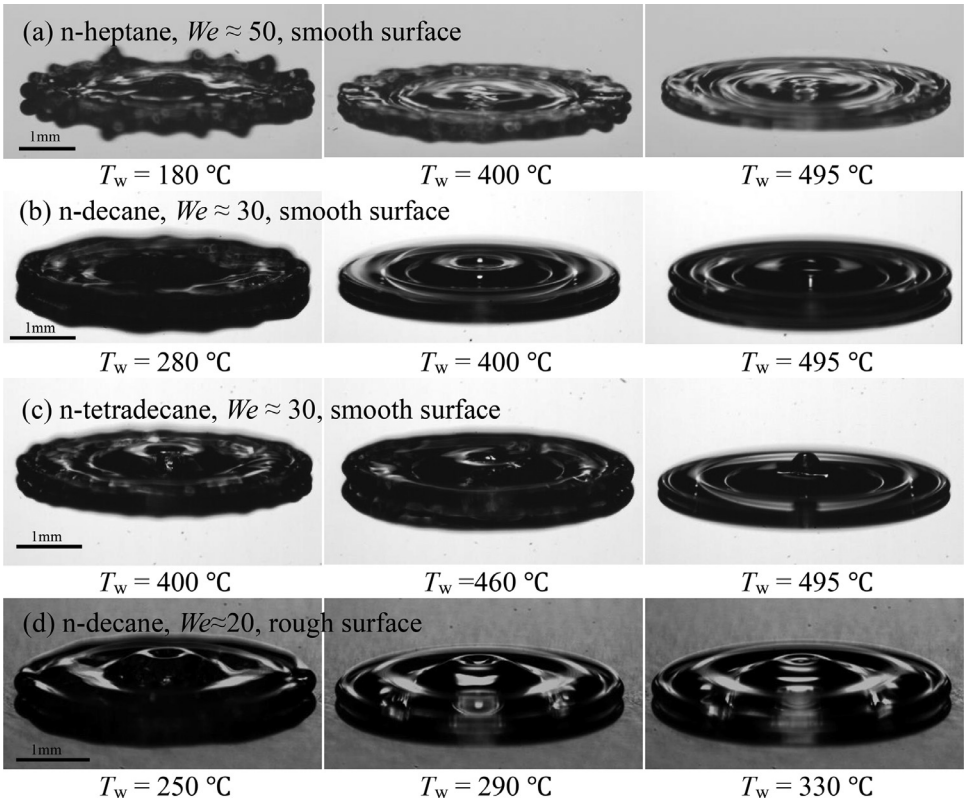

Fig. 9. Images of rim disturbance of n-heptane, n-decane and n-tetradecane droplets at varied T_w at *We* ≈ 20,30 and 50 on smooth and rough surface at t = 3.0 ms.

temperature at 3.0 ms. Finger-like disturbances were observed on the periphery of the lamella for n-heptane droplet at T_w = 180 °C at 3.0 ms as presented in Fig. 9(a), which is different from the images in Fig. 4(e). Previous literature has suggested that the fingering is triggered by the Rayleigh-Taylor instability casued by the decelerating contact line [22]. We found that the formation of the fingering is firstly promoted because the gas density near the contact line is reduced due to the increase in T_w. Then, further increase in T_w results in the decrease of the total contact line length, and as such fingering formation is not favored as presented in Fig. 9(a) at T_w = 495 °C. Consequently, the liquid is levitated completely by the Leidenfrost gas layer, and the fingering formation during the spreading process is mitigated due to the vanishment of the contact line. The rim of the lamella firstly spreads outwards and then recedes over the Leidenfrost gas layer. Similar influence of T_w is also observed for n-decane and n-tetradecane droplet on smooth and rough surface at varied *We* in Fig. 9(b-d). Such fingering disturbance was also observed by Khavari et al. [23] before the transition boiling regime and it was found that the number of fingers increases with *We* and decreases with T_w.

3.2. Spreading dynamics and maximum spreading diameter

3.2.1. Spreading dynamics on varied T_W and roughness

Fig. 10 shows the evolution of non-dimensional spreading diameter, $\beta = D/D_0$, of n-heptane and n-tetradecane droplet impacting on smooth and rough surface with different T_w at different non-dimensional time $\tau = tU_0/D_0$. For n-heptane droplet at *We* ≈ 20 impacting on smooth surface at T_w = 30 °C, the droplet is in evaporation regime, it spreads to a maximum spreading diameter denoted by β_{max} and slightly recoils because of its surface tension. At T_w = 50 °C, the droplet spreads more slowly and reaches a smaller β_{max}, starts recoils, and then oscillates. At T_w = 80 °C and 100 °C, the droplet is in the nucleate boiling regime, it reaches a smaller β_{max} and starts to oscillate later than it does in the evaporation regime because of larger recoil height. At T_w = 170 °C, the droplet is in transition regime and ejects lots of secondary droplets, and the spreading diameter is not smooth compared to that in evaporation and nucleate boiling regime. At T_w = 190 °C, 400 °C and 500 °C, the droplet is in film boiling regime, and it recoils quickly after reaching β_{max} and shows little difference in the evolution of β. Similar trends are also observed for n-heptane droplet on rough surface as presented in Fig. 10(b), except that the droplet is already in film boiling regime at T_w = 170 °C. The time when the droplet reaches β_{max} is defined as τ_{max} as marked in Fig. 10(b). The β evolution ends when the droplet is completely rebounded from the surface at τ_r. The evolution of n-tetradecane droplet spreading on smooth and rough surfaces is presented in Fig. 10(c-d). The droplet oscillates in nucleate boiling and transition boiling regime.

3.2.2. Maximum spreading diameter

The non-dimensional maximum spreading diameter of the spreading lamella, β_{max}, is one of the prominent parameters to describe the morphology of an impacting droplet. Fig. 11(a) shows the variation of β_{max} of n-heptane droplets at different T_w and*We* on smooth surface. Overall, β_{max} increases with *We* from 20 to 70 at different T_w; it decreases with increasing T_w until reaches the film boiling regime, where β_{max} is not strongly influenced by T_w. It is noted that the Leidenfrost temperature marked by the dash line in the present *We* range is barely changed, which is consistent with the literature [24]. The β_{max} for n-heptane droplet at *We* ≈ 70 is slightly increased with increasing T_w in the film boiling regime, which is due to the significant fingering disturbance in the rim.

When the surface is not heated, β_{max} is larger for liquids with smaller viscosity on smooth surfacebecause of less viscous dissipation during the spreading as shown in Fig. 11(b). Then β_{max} decreases with the increase of T_w until it reaches a Leidenfrost temperature T_L. The n-heptane, n-decane and n-tetradecane droplets

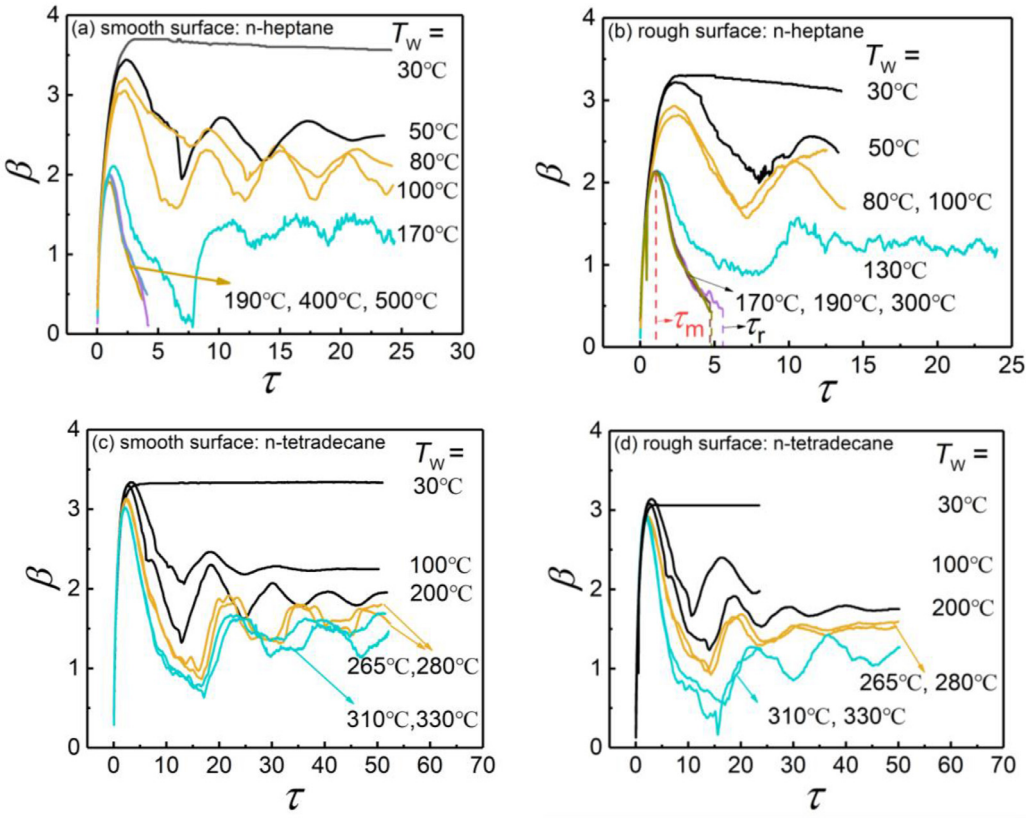

Fig. 10. Non-dimensional spreading diameter β of (a) n-heptane droplets at $We \approx 20$ on smooth surface; (b) n-heptane droplets at $We \approx 20$ on rough surface; (c) n-tetradecane droplets at $We \approx 70$ on smooth surface; (d) n-tetradecane droplets at $We \approx 70$ on rough surface.

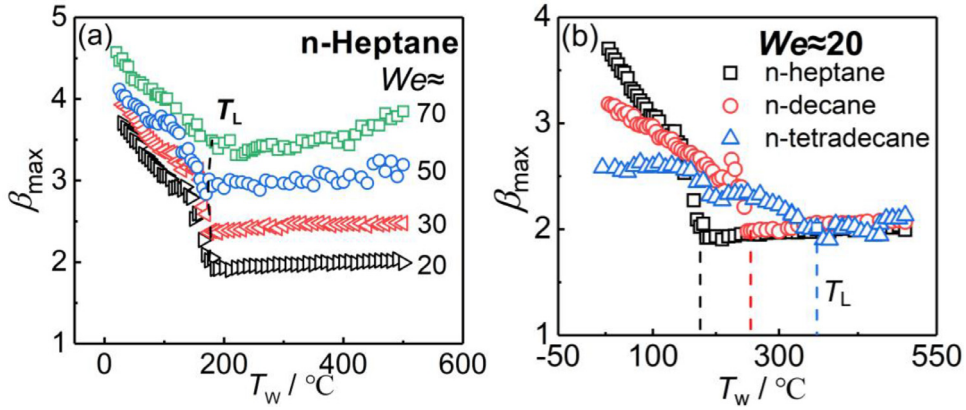

Fig. 11. (a) β_{max} of n-heptane droplets at varied T_w and We on smooth surface. The dynamic Leidenfrost temperatures T_L for n-heptane droplets at $We \approx$ 20,30,50,70 are 175 °C,180 °C,170 °C,180 °C respectively.; (b) β_{max} of n-heptane, n-decane and n-tetradecane droplets at varied T_w at $We \approx 20$ on smooth surface. The error bar for β_{max} is $\pm$ 0.08, which is very small and invisible in the figure.

reach T_L at T_w = 180 °C, 260 °C, and 380 °C respectively. When the surface is not heated, the β_{max} at $We \approx 20$ of n-heptane (μ = 0.41 mPas) is 3.70 and 2.57 for n-tetra-decane (μ = 2.18 mPas). The n-heptane droplet has largest β_{max} when the surface is not heated, thus is mostly influenced by T_w since three liquids eventually reach the same β_{max} at $T_w > T_L$. There is barely any difference for β_{max} of different liquids in the film boiling regime. This is also why β_{max} in the film boiling regime in previous study is only Weber number dependent.

It is well known that surface roughness reduces β_{max} when the surface is not heated because of larger energy dissipation during the spreading [25]. Fig. 12 represents β_{max} of n-heptane droplets on rough and smooth surfaces at $We \approx 20$. It is seen that surface roughness also influences the spreading of droplets on a heated surface. Firstly, β_{max} is smaller on rough surface at $T_w < T_L$ mainly because of larger viscous dissipation during the spreading as discussed comprehensively in the literature [25]. It is noted that the droplet reaches T_L earlier on the rough surface and has a larger β_{max}. A possible explanation is that the cavity in the roughness provides more space for fuel vapor, and it is easier to form a vapor layer to levitate the droplet than the smooth surface, consequently resulting in a larger β_{max}. It is noted that the rough surface provides more nucleation sites which favor the heat transfer from the surface to the droplet. As such, a lower surface temperature is needed to fully levitate the droplet due to faster vapor pressure build up in between, resulting in a lower T_L.

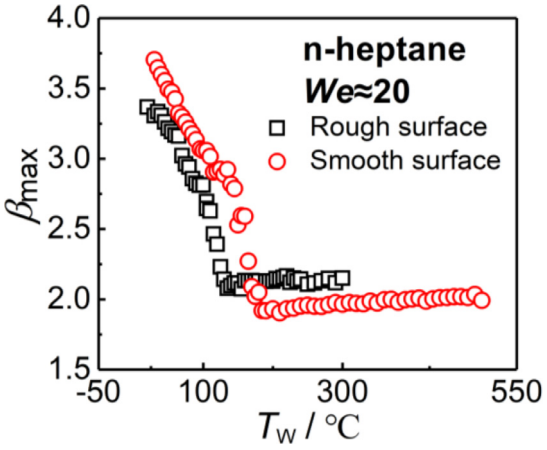

Fig. 12. β_{max} for n-heptane droplets at smooth surface and rough surface at $We \approx 20$.

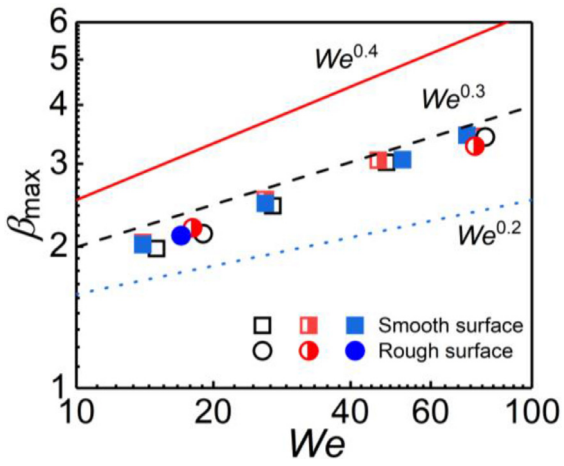

Fig. 13. β_{max} of n-heptane (empty black symbols), n-decane (half-empty red symbols) and n-tetradecane (filled blue symbols) droplets in film boiling regime on smooth and rough surface at varied Weber number. Correlations of β_{max} in film boiling regime from different models [26]. The figure in represented in log format. The error bar for β_{max} is ±0.08, which is very small and invisible in the figure.

The maximum spreading diameter is approximately the same in the film boiling regime as presented in Fig. 11 which is also strongly concerned with multiple models to predict. As shown in Fig. 13, three typical models for β_{max} of droplet impact on heated surface in film boiling regime [26] are compared with the experimental data in this work. Surface roughness is found to slightly increase β_{max} in the film boiling regime as presented in Fig. 12. The data of β_{max} on rough and smooth surface both agree with the scaling $\beta_{max} \sim We^{0.3}$ with the mean error $((\beta_{max\_exp}-\beta_{max\_model})/\beta_{max\_model})$ being 0.07. The scaling component 3/10 is consistent with the model from multiple previous studies [13, 18, 27]. The main assumption of this scaling law is that the spreading of the liquid is driven by the vapor flow underneath the droplet [9]. Similar stainless steel surface with surface roughness R_a less than 0.05μm was used by Liang et al. [18].

3.3. Droplet bouncing in film boiling regime

3.3.1. Bouncing height

When the droplet reaches the film boiling regime, the non-dimensional spreading diameter β is barely changed as shown in

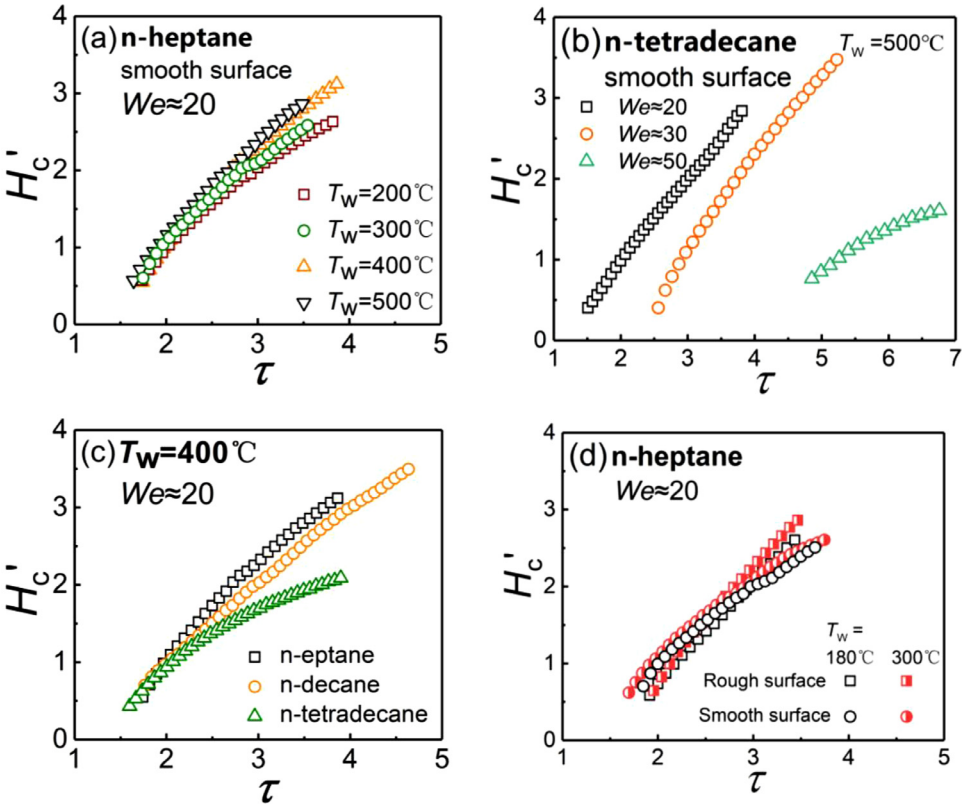

Fig. 14. Non-dimensional droplet central height $H_c'=H_cU_0/D_0$ for (a) n-heptane at $We \approx 20$ on smooth surface at varied T_w; (b) n-tetradecane droplet at $T_w = 500$ °C on smooth surface at $We \approx 20$,30 and 50; (c) n-heptane, n-decane and n-tetradecane droplet at $T_w = 400$ °C on smooth surface at $We \approx 20$; (d) n-heptane droplet on smooth and rough surface at $We \approx 20$ at $T_w = 180$ and 300 °C.

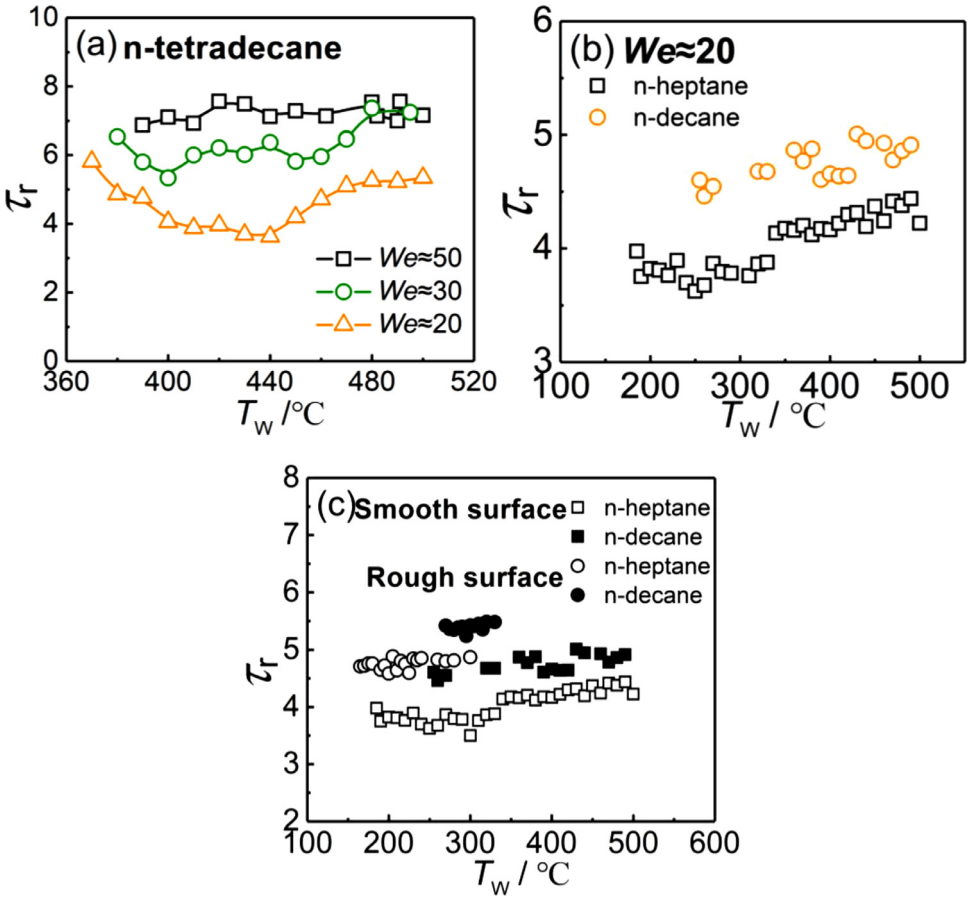

Fig. 15. (a) Non-dimensional residence time $\tau_r = t_r U_0/D_0$ for n-tetradecane at varied T_w and *We* on smooth surface; (b) τ_r for n-heptane and n-decane droplets at varied T_w on smooth surface; (c) τ_r for n-heptane and n-decane droplets with varied T_w at $We \approx 20$ on smooth and rough surface.

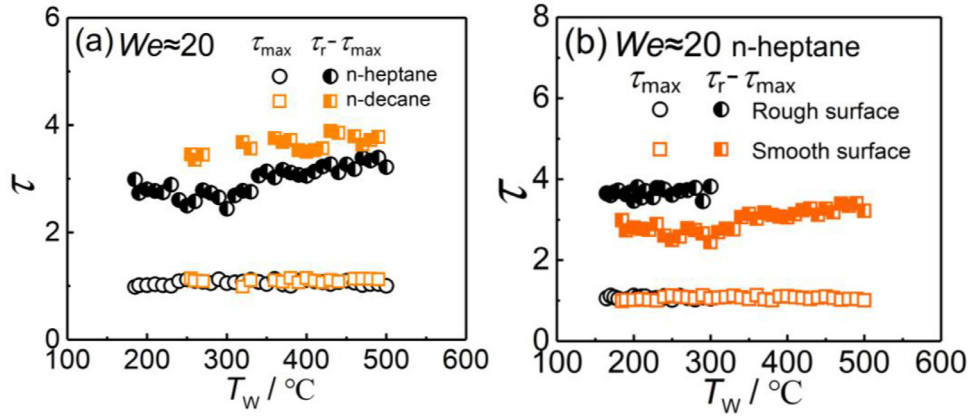

Fig. 16. (a) Non-dimensional maximum spreading time τ_{max} and recoil time (τ_r -τ_{max}) for n-heptane and n-decane at $We \approx 20$ on smooth surface. (b) Non-dimensional maximum spreading time τ_{max} and recoil time (τ_r -τ_{max}) for n-heptane droplet at $We \approx 20$ on rough and smooth surface.

Fig. 10. Fig. 14 shows the non-dimensional height of the droplet center H_c' ($H_c U_0/D_0$) during the rebound in the film boiling regime with varied T_w at varied *We* on smooth and rough surface. With the increase of T_w, the higher vapor pressure makes the droplet rebound faster and increase H_c' at the same time as presented in Fig. 14(a). Larger *We* leads to larger β_{max} as presented in Fig. 11, and longer time for the droplet to rebound as shown in Fig. 14(b), which has also been observed by Gastanet et al. [11].

For liquids with varied viscosity, although they have almost same β_{max} when the droplet reaches T_L in film boiling regime as presented in Fig. 11, the n-tetradecane with larger viscosity still rebound slower than n-heptane with smaller viscosity as shown in Fig. 14(c). The droplet is inertial driven during the spreading which is barely influenced by viscosity. Viscosity begins to play a role during the rebound driven by capillary pressure and consequently higher viscosity results in slower rebound and smaller central height at the same time. The surface roughness slightly in-

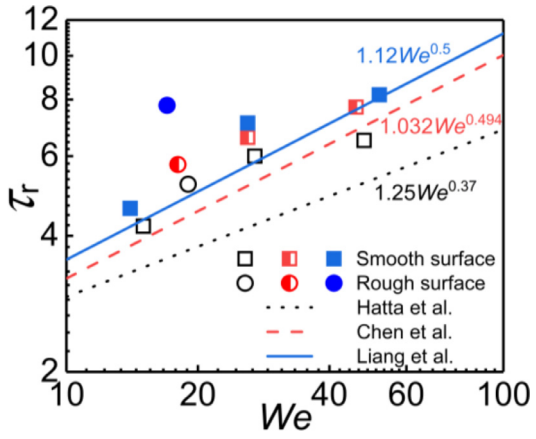

Fig. 17. τ_r of varied droplets at different *We* on smooth and rough surface. Correlations of τ_r from different models. Hatta et al. [29]: $\tau_r \sim 1.25We^{0.37}$; Chen et al. [28]: $\tau_r \sim 1.12We^{0.5}$; Liang et al. [18]: $\tau_r \sim 1.032We^{0.494}$.
Black open symbols: n-heptane; red half-open symbols: n-decane; blue solid symbols: n-tetradecane.

fluences β_{max} as presented in Fig. 12 and also slightly effect H_c' as shown in Fig. 14(d).

3.3.2. Residence time

Fig. 15(a) shows the non-dimensional residence time $\tau_r = t_r U_0/D_0$ for n-tetradecane droplet at varied T_w and *We* on smooth surface. It takes a shorter time for the droplet to rebound when *We* is small. It is noted that most previous studies assumed that residence time is only related to *We* [18, 28, 29]. However, τ_r is found to be also influenced by liquid viscosity as shown in Fig. 15(b) and surface roughness in Fig. 15(c). It takes a longer time to rebound for liquids with larger viscosity and on surface with larger roughness.

To understand the experimental observations, we split the residence time (τ_r) into the spreading time (τ_{max}) that the droplet reaches the β_{max} and the recoil time (τ_r-τ_{max}) as shown in Fig. 16(a). It turns out that the droplet takes the same time to spread to the same β_{max} but different times to recoil. The droplet dynamics is dominated by impact inertia during the spreading because of the large Reynolds number. Therefore it shows no difference with a vapor layer underneath to prevent the contact with the surface. But viscosity begins to play a role during the rebound driven by capillary pressure, and consequently a higher viscosity eventually results in larger residence time τ_r.

We also analyzed the residence time for different surface roughness in Fig. 16(b), which shows that the difference also roots in the recoil stage. All these results suggest that both surface roughness and liquid viscosity affect the residence time of the bouncing droplet and need to be considered in modeling.

Above all the discussion about spreading and rebound process, residence time τ_r is strongly concerned with multiple models to predict [18, 28, 29]. As shown in Fig. 17, the resident time is influenced by the liquid viscosity and surface roughness, thus the models that don't contain liquid viscosity and surface roughness will not be able to give good prediction. Such comparison indicates that liquid viscosity and surface roughness should be considered in residence time modeling in the future work.

4. Conclusion

With the increasing interest in engine downsizing and in considering the strong relation between the spray impingement and droplet-solid surface interaction, we have comprehensively investigated the thermo hydrodynamic behaviors of droplet impact at *We* ≈ 20~70 on solid surface. The particular emphasis of the study was on the effect of droplet viscosity, the surface roughness and temperature on droplet spreading and bouncing, bubble generation, spreading rim disturbance and the spreading and bouncing dynamics.

1 Four typical regimes of droplet impact on heated surface are identified. Bubbles generated inside the droplet at $T_w > T_b$ are observed. More and larger bubbles are generated with increasing T_w in nucleate boiling and transition boiling regime. No bubbles are formed in film boiling regime. The rim is smoother with weaken rim disturbance with the increase of T_w.
2 The droplet oscillates in terms of spreading and contracting for $T_L > T_w > T_b$, as identified by the spreading diameter (β) oscillates as a function of time. However, for $T_w > T_L$, the β evolution shows barely difference in film boiling regime. The maximum non-dimensional diameter β_{max} decreases with increasing T_w until a dynamic Leidenfrost temperature T_L is reached. The liquid viscosity decreases β_{max} when the surface is not heated and shows no effect in film boiling regime.
3 Liquids with larger viscosity takes longer time to recoil and eventually result in larger residence time τ_r. The residence time is not only significantly increased with increasing Weber number, but also increased with larger liquid viscosity and surface roughness, which should be considered in future model of residence time.

The present results are expected to provide useful guidance in the development of spray dynamic models and the design of next-generation, down-sized engines.

Declaration of Competing Interest

None.

CRediT authorship contribution statement

Mengxiao Qin: Data curation, Formal analysis. **Yang Guo:** Writing - review & editing. **Chenglong Tang:** Conceptualization, Methodology, Resources. **Peng Zhang:** Methodology, Resources. **Zuohua Huang:** Writing - review & editing.

Acknowledgement

The work at Xi'an Jiao Tong University was supported by National Natural Science Foundation of China (91941101, and 51722603), and Open Research Fund of Beijing Key Laboratory of Powertrain for New Energy Vehicle, Beijing Jiaotong University. The work at The Hong Kong Polytechnic University was supported by GRC/GRF (PolyU 152651/16E) and PolyU CRG (G-YBXN). MXQ was additionally supported by the Joint PhD Supervision Scheme of the Hong Kong Polytechnic University (G-SB1Q).

Supplementary materials

Supplementary material associated with this article can be found, in the online version, at doi:10.1016/j.ijheatmasstransfer.2020.120076.

Reference

[1] S. Nukiyama, The maximum and minimum values of the heat Q transmitted from metal to boiling water under atmospheric pressure, Int. J. Heat Mass Transfer 9 (12) (1966) 1419–1433.
[2] S. Chandra, C.T. Avedisian, On the Collision of a Droplet with a Solid Surface, in: Proc. R. Soc. A, 432, 1991, pp. 13–41.
[3] J.D. Bernardin, C.J. Stebbins, I. Mudawar, Mapping of impact and heat transfer regimes of water drops impinging on a polished surface, Int. J. Heat Mass Transfer 40 (2) (1997) 247–267.

[4] J.D. Naber, P.V. Farrell, Hydrodynamics of droplet impingement on a heated surface, SAE Trans., (1993) 1346-1361.
[5] A.L.N. Moreira, A.S. Moita, M.R. Panão, Advances and challenges in explaining fuel spray impingement: how much of single droplet impact research is useful? Prog. Energy Combust. Sci. 36 (5) (2010) 554–580.
[6] H.M. Kwon, J.C. Bird, K.K. Varanasi, Increasing Leidenfrost point using micro–nano hierarchical surface structures, Appl. Phys. Lett. 103 (20) (2013) 201601.
[7] D. Orejon, K. Sefiane, Y. Takata, Effect of ambient pressure on Leidenfrost temperature, Physical Review E 90 (5–1) (2014) 053012.
[8] V. Bertola, An impact regime map for water drops impacting on heated surfaces, Int. J. Heat Mass Transfer 85 (2015) 430–437.
[9] T. Tran, H.J. Staat, A. Prosperetti, C. Sun, D. Lohse, Drop impact on superheated surfaces, Phys. Rev. Lett. 108 (3) (2012) 036101.
[10] A.-l. Biance, F. Chevy, C. Clanet, G. Lagubeau, D. Quéré, On the elasticity of an inertial liquid shock, J. Fluid Mech. 554 (2006) 47–66.
[11] G. Castanet, O. Caballina, F. Lemoine, Drop spreading at the impact in the Leidenfrost boiling, Phys. Fluids 27 (6) (2015) 063302.
[12] S. Fukuda, M. Kohno, K. Tagashira, N. Ishihara, S. Hidaka, Y. Takata, Behavior of Small Droplet Impinging on a Hot Surface, Heat Transfer Eng 35 (2) (2013) 204–211.
[13] T. Tran, H.J.J. Staat, A. Susarrey-Arce, T.C. Foertsch, A. van Houselt, H.J.G.E. Gardeniers, A. Prosperetti, D. Lohse, C. Sun, Droplet impact on superheated micro-structured surfaces, Soft Matter 9 (12) (2013) 3272–3282.
[14] P. Zhao, G.K. Hargrave, H.K. Versteeg, C.P. Garner, B.A. Reid, E.J. Long, H. Zhao, The dynamics of droplet impact on a heated porous surface, Chem. Eng. Sci. 190 (2018) 232–247.
[15] E.-S.R. Negeed, M. Albeirutty, S.F. Al-Sharif, S. Hidaka, Y. Takata, Dynamic Behavior of a Small Water Droplet Impact Onto a Heated Hydrophilic Surface, J, Heat Transfer 138 (4) (2016) 042901.
[16] W. Zhang, T. Yu, J. Fan, W. Sun, Z. Cao, Droplet impact behavior on heated micro-patterned surfaces, J, Appl. Phys. 119 (11) (2016) 114901.
[17] M. Qin, C. Tang, S. Tong, P. Zhang, Z. Huang, On the role of liquid viscosity in affecting droplet spreading on a smooth solid surface, Int. J. Multiphase Flow 117 (2019) 53–63.
[18] G. Liang, S. Shen, Y. Guo, J. Zhang, Boiling from liquid drops impact on a heated wall, Int. J. Heat Mass Transfer 100 (2016) 48–57.
[19] L.R. Villegas, S. Tanguy, G. Castanet, O. Caballina, F. Lemoine, Direct numerical simulation of the impact of a droplet onto a hot surface above the Leidenfrost temperature, Int. J. Heat Mass Transfer 104 (2017) 1090–1109.
[20] G.D. W., P.R. H., Perry's Chemical Engineers Handbook, McGraw-Hill, New York.., 2008.
[21] S.T. Thoroddsn, T.G. Etoh, K. Takehara, N. Ootsuka, Y. Hatsuki, The air bubble entrapped under a drop impacting on a solid surface, J, Fluid Mech 545 (545) (2005) 203–212.
[22] C. Josserand, S.T. Thoroddsen, Drop Impact on a Solid Surface, Annu. Rev. Fluid Mech. 48 (2016) 365–391.
[23] M. Khavari, C. Sun, D. Lohse, T. Tran, Fingering patterns during droplet impact on heated surfaces, Soft Matter 11 (17) (2015) 3298–3303.
[24] H.J.J. Staat, T. Tran, B. Geerdink, G. Riboux, C. Sun, J.M. Gordillo, D. Lohse, Phase diagram for droplet impact on superheated surfaces, J, Fluid Mech 779 (2015) R3.
[25] C. Tang, M. Qin, X. Weng, X. Zhang, P. Zhang, J. Li, Z. Huang, Dynamics of droplet impact on solid surface with different roughness, Int. J. Multiphase Flow 96 (2017) 56–69.
[26] G. Liang, I. Mudawar, Review of drop impact on heated walls, Int. J. Heat Mass Transfer 106 (2017) 103–126.
[27] H. Nair, H.J. Staat, T. Tran, A. van Houselt, A. Prosperetti, D. Lohse, C. Sun, The Leidenfrost temperature increase for impacting droplets on carbon-nanofiber surfaces, Soft Matter 10 (13) (2014) 2102–2109.
[28] R.H. Chen, S.-L. Chiu, T.-H. Lin, Resident time of a compound drop impinging on a hot surface, Appl. Therm. Eng. 27 (11–12) (2007) 2079–2085.
[29] N. Hatta, H. Fujimoto, K. Kinoshita, H. Takuda, Experimental Study of Deformation Mechanism of a Water Droplet Impinging on Hot Metallic Surfaces Above the Leidenfrost Temperature, J, Fluids Eng 119 (3) (1997) 692.